Full length article

Influence of nanoscale structural heterogeneity on shear banding in metallic glasses

Pengyang Zhao [a], Ju Li [b, c], Jinwoo Hwang [a, **], Yunzhi Wang [a, *]

[a] *Department of Materials Science and Engineering, The Ohio State University, 2041 College Road, Columbus, OH 43210, USA*
[b] *Department of Nuclear Science and Engineering, Massachusetts Institute of Technology, 77 Massachusetts Avenue, Cambridge, MA 02139, USA*
[c] *Department of Materials Science and Engineering, Massachusetts Institute of Technology, 77 Massachusetts Avenue, Cambridge, MA 02139, USA*

ARTICLE INFO

ABSTRACT

Structural heterogeneity at the nanoscale such as medium-range order (MRO) in metallic glasses (MGs) has been suggested by theories and simulations for many years and recently been observed by experiments. However, its correlation with plastic deformation is still poorly understood and investigation into this correlation has just begun. In this study, we first propose a correlation between the properties of shear transformation zone (STZ) and the local structural information at the MRO length scale. As revealed by experiments, the MRO exhibits different types of atomic order and symmetry in MGs depending strongly on the processing history and service condition. We then carry out STZ dynamics simulations to document effects of volume fraction and symmetry of dissimilar STZs (derived from experimental characterization of the MRO) on shear banding dynamics and stress-strain behavior. In particular, a "precipitation-hardening" effect is observed and "strain frustration" is introduced to explain and better understand the influence of nanoscale structural heterogeneity on mechanical behavior of MGs. Our approach intends to provide new fundamental insights into the relationship between the mechanical properties of MGs and their MRO-level structural heterogeneities.

© 2017 Acta Materialia Inc. Published by Elsevier Ltd. All rights reserved.

1. Introduction

Various structural heterogeneities have been introduced in metallic glasses (MGs) in order to tune their mechanical properties, with the primary goal of improving their tensile ductility without sacrificing much of the strength. For instance, MG-matrix composites containing a crystalline phase in the forms of isolated dendrites ($\sim 10\,\mu$m) [1—3], nanocrystals (~ 5 nm) [4,5], and crystalline-amorphous multilayers [6] have been produced to show some improvement in tensile ductility; hierarchical MG composites exhibiting two length scales of heterogeneities (from ~ 10 nm to ~ 100 nm) have also been obtained through phase separation [7]; MG foams are even produced as strong and lightweight materials for certain applications [8]. The diverse scales of these structural heterogeneities have shown some interesting and promising effects on the formation of shear bands at room temperature and may indeed provide ways of controlling plasticity in MGs, similar to the roles played by homo- and/or hetero-phase interfaces in plastic deformation of crystals. However, the characteristic length scale of the above heterogeneities are all well above the size of the so-called medium-range order (MRO), which resides at ~ 1 nm and has been considered as one of the key elements of intrinsic glass structures [9—15]. Using fluctuation electron microscopy, Hwang et al. [14] have recently revealed a crystal-like MRO in $Zr_{50}Cu_{45}Al_5$ MG, which has an average size of ~ 1 nm, similar to those found in some molecular dynamics (MD) simulations (e.g., [16,17]). In addition, it has been shown that this crystal-like MRO would transform into another type of MRO containing a chain of icosahedral nearest-neighbor clusters upon annealing [14]. Since the ductility and strength of MGs can also be significantly altered upon annealing [18], it is natural to ask if these nanoscale structural heterogeneities are indeed responsible for the change of properties. Such correlation, if it exists, will certainly distinguish itself from the "structure-property" relationships discussed at the very beginning because the MRO occurs at a much smaller length scale and are believed to be *intrinsic* in the sense that they may be strongly related to the thermal and/or service history of a glass, offering a

* Corresponding author.
** Corresponding author.
  E-mail addresses: hwang.458@osu.edu (J. Hwang), wang.363@osu.edu (Y. Wang).

different strategy of tailoring the property of MGs.

So far, all MROs revealed either experimentally or computationally have a length scale (~ 1 nm) commensurate with the size of the shear transformation zone (STZ) [19–22] that is considered as the fundamental plasticity carrier in MGs [19,23–25] (and may also correlate with the structural relaxation [26–28]). If MRO indeed plays a key role in the "structure-property" correlation of MGs, it is reasonable to expect that there should be a direct correlation between the MRO structure and the STZ behavior as they spatially "coincide" with each other owing to the comparable length scales. The existence of nanoscale structural heterogeneities (spatially distributed MROs) may imply that the nature of STZ events can be quite different, depending on whether they are activated in normal glassy regions or regions containing MROs. In fact, recent molecular dynamics (MD) simulations [29,30] have suggested that vibrational "soft spots" (certain structural heterogeneities) are fertile sites for the initiation of STZs. Those structural soft spots are composed of or centered around the so-called "geometrically unfavored motifs" (GUMs) that are distinctively different from the dominant structural unit in MGs, i.e., the full icosahedra that are the most energetically favorable and geometrically comfortable short-range order (SRO) motifs. It was further suggested that in the potential energy landscape of MGs, "basins" with a smaller local curvature (corresponding to GUMs) tend to have lower barriers for transitions to neighboring basins [30].

The GUM-STZ correlation revealed by Ding et al. [30], though statistical in nature, indeed provides some atomistic basis on exploring the "structure-property" relationship by focusing on the intrinsic structural heterogeneities at the MRO level. A recent continuum simulation showed that plasticity and toughness of MGs could be enhanced by introducing free volume dispersion [31], though the heterogeneity was limited to the continuum finite-element mesh size that is much larger than MRO. An interesting question that remains unexplored so far is whether the experimentally revealed MROs can in fact correlate with the observed macroscopic mechanical properties of MGs. We thus hypothesize here that the inherent local structural heterogeneity in MGs will bring regions (~ 1 nm) of the glass corresponding to the presence of MROs into distinctive internal states as compared to the rest of the glass. More specifically, STZs resulting from regions containing crystalline-like MROs [14,17] are likely to have quite different transformation pathways (e.g., shear modes and activation energy barriers), as also suggested in Ref. [30]. In this paper, we will test this hypothesis to correlate MROs and STZs, which has been missing in all previous STZ dynamics simulations [32–35], and explore the resulting impact on shear banding and stress-strain behaviors in MGs. It will be shown that by increasing dissimilar STZs derived from the experimentally informed MROs, shear banding and stress-strain curves are significantly changed and an effect similar to "precipitation-hardening" in crystalline solids is observed in MGs.

2. Methods

2.1. Influence of MROs on STZ operations: experimental findings and theoretical basis

Crystal-like ordering (e.g., FCC type) at a length scale of ~ 1 nm has been observed frequently in MGs [14,36–39]. The effect of microalloying in controlling those nanoscale ordering has also been demonstrated [40]. In addition to those experimental studies, a recent *ab initio* MD simulation study combined with a genetic algorithm also revealed an FCC motif in MGs [41]. Considering that the current atomistic/*ab initio* simulations tend to have too high of a cooling rate that artificially boosts 5-fold icosahedra count, the

crystalline motif count in real MGs may actually be even higher than that suggested by the simulation results. The formation of nanocrystals in MGs [42] may further suggest that there is an inherent structural correlation between glasses and (nanoscale) crystals.

Owing to the distinctively different structural features between the MROs (with crystalline order) and the glassy matrix (with icosahedral order), the corresponding STZs are likely to exhibit different characteristics as well. The property difference resulted from compositional and processing-condition differences in MGs are generally believed to be tied to MROs, which calls for more experimental and theoretical studies [43]. On the other hand, the properties of MG composites embedded with nanocrystals ($1 - 10$ nm) have been explored by experiments [4,5,44], which show the significant role of those nanocrystals in altering shear banding. Although MROs are not nanocrystals, its crystal-like symmetry is expected to render some special crystal-like planes and thus lead to dissimilar STZs from those of the glassy matrix. In fact, the strong influence of local atomic arrangements on STZ operations has long been suggested [25]. We can take the free volume as an example to illustrate the influence of structural order on the underlying defects. In crystals, the free volume will be localized as a 0-dimensional defect, i.e., vacancy, which plays a central role in determining the physical properties of crystals. However, a hole of atomic size is found unstable in glass by simulations [45], which is later confirmed by direct experimental measurement of the free volume in MGs [46]; instead, other concept such as the "connected atomistic free volume" [35] should be used to better define the free volume in glass. The fundamental physics behind this is that a crystal lattice tends to preserve sites while MGs do not. Following the tenet that "microstructure determines properties", the effect of dissimilar STZ operations due to the presence of MROs should be of great significance to establish a "structure-property" relationship in MGs and deserves theoretical explorations.

2.2. Incorporating MROs in STZ dynamics

To investigate the correlation between MROs and shear banding, a model that can bridge the length and time scales between individual STZ events and the formation of shear bands is necessary. To this end, we employ our previously developed heterogeneously randomized STZ model [33,35], which allows mesoscale simulations of plastic deformation of MGs using STZ as the building block, and introduce new types of STZ that are informed by the experimentally revealed MROs (Fig. 1(b)) [14]. While it is still challenging at this moment to determine the property difference between different types of MROs and STZs (which will be defined more clearly later), the apparent atomic packing symmetry difference as shown by the experiments (Fig. 1) may lead to different plastic responses when relaxing local stresses via STZ transformations.

In theory, STZ resulted from regions containing "crystal-like" structures (Fig. 1(b)) may "see" a relatively well-defined lattice plane over ~ 1 nm and consequently resemble some features of plastic slip in crystals when activated, which is quite different from STZs resulted from regions of full icosahedra. This can be better understood by adopting the concept of generalized-stacking fault (GSF) energy profile in MGs [47]. As schematically shown in Fig. 1(c), if STZ occurs in matrix regions rich in icosahedral clusters, we should expect an initially high activation energy barrier (between A_0 and A_1) corresponding to the first STZ transformation, which should relate to typical MG properties such as high elastic limit and high yield strength [48]. The energy barriers for the subsequent STZ transformations (between A_1 and A_2) are, however, expected to be much lower due to softening [33]. If plastic shear is accommodated by STZs at regions containing crystal-like MROs,
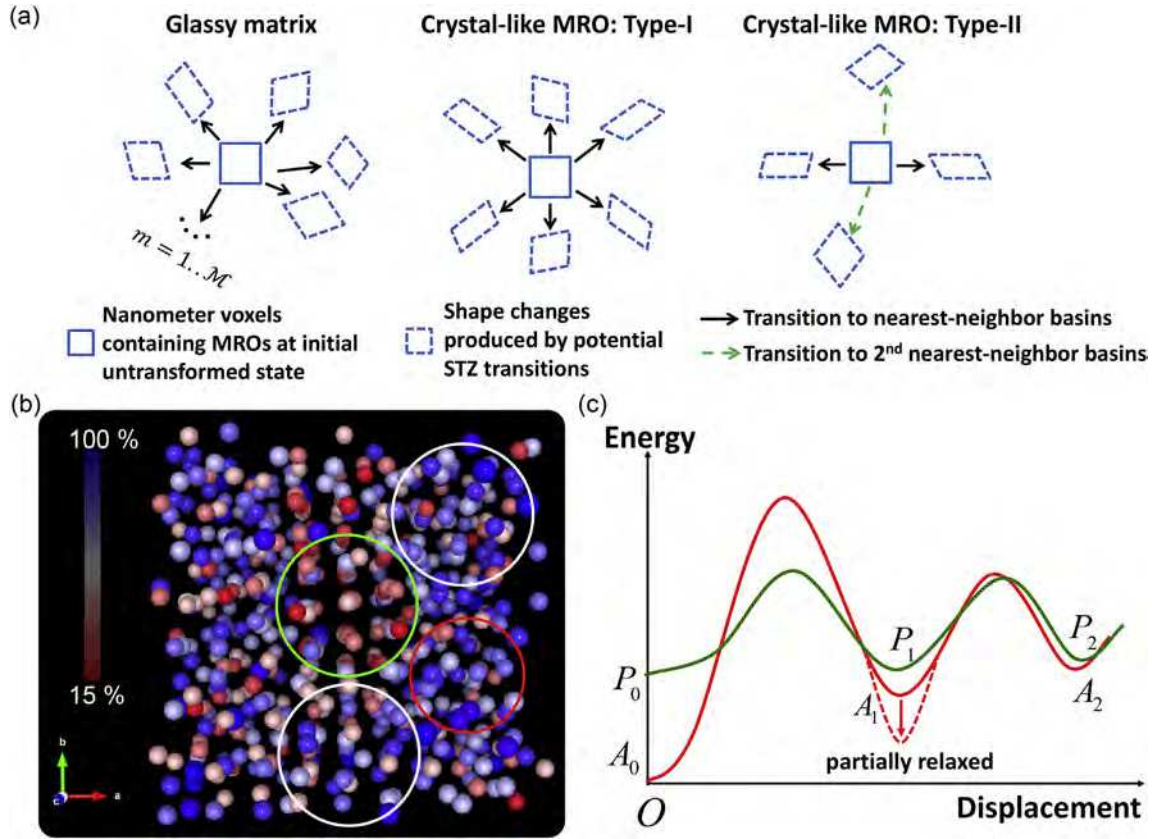
Fig. 1. (a) Illustration of different types of STZs having different shear modes, which is motivated by (b) experimentally revealed MROs including pseudo six-fold crystal-like MRO (green circle), two-fold aligned icosahedral MRO (white circles), and random icosahedra rich glassy matrix (red circle) [14]. Atoms are colored by the fraction of pentagons in their Voronoi Polyhedra. (c) Schematics of GSF energy of a MG as a function of a sharp displacement discontinuity when shear is accommodated either by glassy STZs (red curve) or by crystal-like STZs (green curve). (For interpretation of the references to colour in this figure legend, the reader is referred to the web version of this article.)

e.g., the two types illustrated in Fig. 1(a), we may expect a crystal-like GSF energy profile as typically seen in crystals, which is also illustrated in Fig. 1(c).

In order to explore the above correlation between nanoscale structural heterogeneity (MRO) and STZ, we take a heuristic approach by introducing two types of new STZs (hereafter referred to as crystal-like STZs) into our previous two-dimensional (2D) model [49]. The first type (simply called *six-fold* STZs) resembles the pseudo-FCC symmetry in 2D and its shear modes are predominantly dictated by an event catalog that favors shearing along one of the three "close-packing" planes, similar to the Schmid's law in crystal plasticity. The other type (simply called *two-fold* STZs) are expected to behave in a similar way, but with more limited number of preferential shear directions. More specifically, we assume that there are $M = 6$ shear modes for the six-fold STZs and $M = 2$ modes for the two-fold STZs, as compared to $M = 20$ [33] for the glassy matrix STZs. In our STZ model, each shear mode is described by a stress-free-transformation-strain (SFTS) tensor, which in 2D can be represented as [33]

$$\varepsilon = \begin{bmatrix} \varepsilon_1 & \varepsilon_3 \\ \varepsilon_3 & -\varepsilon_1 \end{bmatrix} \quad (1)$$

To study the influence of crystal-like symmetry, we assume that for a given six-fold STZ, the SFTS tensor of mode-i and mode-j are related by

$$\varepsilon^{(j)} = \mathbf{R}^T \left(\varepsilon^{(i)} + \delta\varepsilon \right) \mathbf{R}, \quad (2)$$

where

$$\delta\varepsilon = \begin{bmatrix} \delta\varepsilon_1 & \delta\varepsilon_3 \\ \delta\varepsilon_3 & -\delta\varepsilon_1 \end{bmatrix} \quad (3)$$

represents the inherent structural fluctuation in glass and the rotation matrix is given by

$$\mathbf{R} = \begin{bmatrix} \cos\theta & -\sin\theta \\ \sin\theta & \cos\theta \end{bmatrix} \quad (4)$$

with a rotation angle

$$\theta = (j - i)\frac{\pi}{3} + \delta\theta. \quad (5)$$

Here $\delta\theta$ represents the structural fluctuation due to the fact that the crystal-like symmetry in the MRO regions is only held approximately. In our simulations, $\delta\varepsilon$ and $\delta\theta$ are drawn from a uniform distribution to account for a relative $\sim 20\%$ variation, which is arbitrarily chosen for the current parametric study. The specification of the SFTS tensors follows the numerical approach presented in Ref. [33] such that the orientation of the crystal-like STZs are isotropically randomized in space. Given the total number of STZ modes $M(\mathbf{x})$ together with the SFTS tensors $\{\varepsilon^{(i)}\}_{i=1}^{M}$, a remaining key parameter to be determined is the corresponding activation
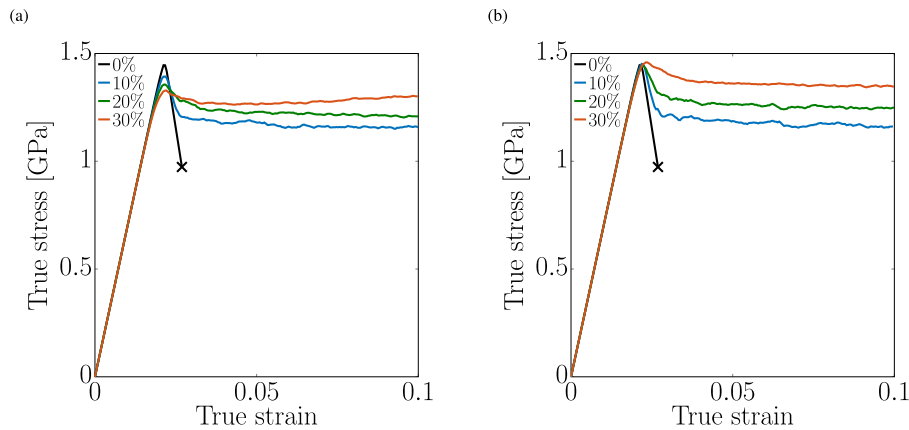
Fig. 2. Simulated tension stress-strain curves of MG samples with different volume fractions of (a) six-fold and (b) two-fold STZs.

energy barrier ΔF^* along each STZ transformation pathway. While the absolute value of ΔF^* ($1 \sim 5\text{eV}$) is still difficult to determine, the more important thing for our study is the difference in ΔF^* between the glassy and crystal-like STZs. It is likely that the latter is lower as the local crystalline order of MROs must lead to some special crystal-like (or less perturbed/interrupted) atomic planes and thus may facilitate slip (along certain directions) more readily due to the inherent (local) translational symmetry, which is not present in the 5-fold icosahedra. Nevertheless, the actual MRO energetics can be complicated and, in this study, we will explore the resulting effect on shear banding via parametric study. In addition, when the embedded crystal-like STZ is sheared by a Burgers vector, because of the amorphous nature at the "precipitate"/matrix interface, it is possible that the "dislocation" can be easily absorbed, similar to the "sink" role played by grain boundaries (amorphous in nature) in crystal plasticity [50]. The energy of the crystal-like STZ after such shearing maintains the same and there is no volume expansion (damage accumulation). In other words, the dissimilar STZs associated with MROs may present "persistence of shear" as in crystals due to site preservation of the crystal-like MRO structure, which is, however, absent in an icosahedron or something that is irregular in terms of translational (slip) operation. As a result, ΔF^* for the crystal-like STZs is assumed to be fixed in our model.

We use a computational grid of 512×1024 where each grid-point represents a coarse-grained (2D) voxel with the size of STZ, which is taken as $1.7 \text{ nm} \times 1.7 \text{ nm}$ in current simulations. This gives the physical length of our computational grid as $0.87 \,\mu\text{m} \times 1.74 \,\mu\text{m}$. (For more details of the model framework, the readers are referred to [33].) The volume fraction of the crystal-like MROs (i.e., the six-fold or two-fold STZs) can be obtained from fluctuation electron microscopy experiments [14,51]. Although the fluctuation electron microscopy can also acquire the spatial distribution of MRO, such data have not been reported in the previous works [14,51]. In the current study, for simplicity, a spatially uniform distribution is assumed for the position of crystal-like STZs. In addition, the elastic modulus of the crystal-like STZs are assumed to be the same as that of the glassy STZs to avoid numerical complexity associated with using the inhomogeneous elasticity solver [35]. Setting the activation energy barrier of 4 eV for the glassy STZs and 3 eV for the crystal-like STZs (other scenarios will be explored in the Discussion section), 69.46 GPa for Young's modulus and 0.365 for Poisson's ratio (assuming isotropic elasticity), various simulations are then carried out in a parametric manner to study possible correlations between MROs and mechanical properties of MGs.

3. Results

Fig. 2(a) shows the stress-strain curves (under uniaxial tension) of the MG samples containing different volume fractions, Φ, of six-fold STZs. In the case of $\Phi = 0\%$, after the peak stress is reached at $\sim$ 2% elongation, significant softening takes place, which corresponds to quick formation of a sharp shear band in the deformation microstructure shown in Fig. 3(a). We will refer to this $\Phi = 0\%$ sample as the "homogeneous[1] sample" hereafter to emphasize that it contains only glassy STZs. It is shown in Fig. 3(a) where significant shear localization occurs within a narrow shear band exhibiting a width of $\sim$ 20 nm. It is also interesting to see that along this shear band, there is a region that experiences much larger plastic deformation as compared to the rest in the band. This "hot region" appears narrower than the rest part of the band. A close inspection of the temporal evolution of the strain maps confirms that this "hot region" corresponds to the initiation sites of the shear band. The corresponding stress map shown in Fig. 3(e) suggests that within the shear band severe stress concentration occurs.

As more and more crystal-like MROs are introduced in the sample, the peak stress gradually decreases with the following softening becoming less and less abrupt; in the case of $\Phi = 30\%$, strain-hardening exists even after the post-peak stress softening (Fig. 2(a)), which has also been observed in some experiments [52]. It needs to be pointed out that "hardening" here refers to the post-peak flow stress, which corresponds to a quasi-steady (STZ-mediated) flow state in our model without considering any failure mechanism. From the corresponding strain maps shown in Fig. 3(b)-(d), it is evident that shear bands become much more diffuse as compared to those observed in the homogeneous sample, with more or less an overall homogeneous deformation in the case of $\Phi = 30\%$. Fig. 4(a) plots the peak stress together with the subsequent stress drop against the six-fold STZ vol.%. These results suggest that the presence of six-fold STZs may simultaneously decrease the strength but prevent catastrophic failure by making shear bands more diffuse and leading to more homogenized deformation.

Since the experiments [14] show that upon annealing, the pseudo-FCC crystal-like MROs can relax into two-fold chains of icosahedral clusters and it is well-known that annealing can increase the strength of MGs but make them more brittle, we

---

[1] This term should not be confused with the fact that our STZ dynamics model is inherently heterogeneous in space and time [33], and the reader is referred to [35] for more discussion on the physical meaning of such idealized glass with $\Phi = 0\%$.
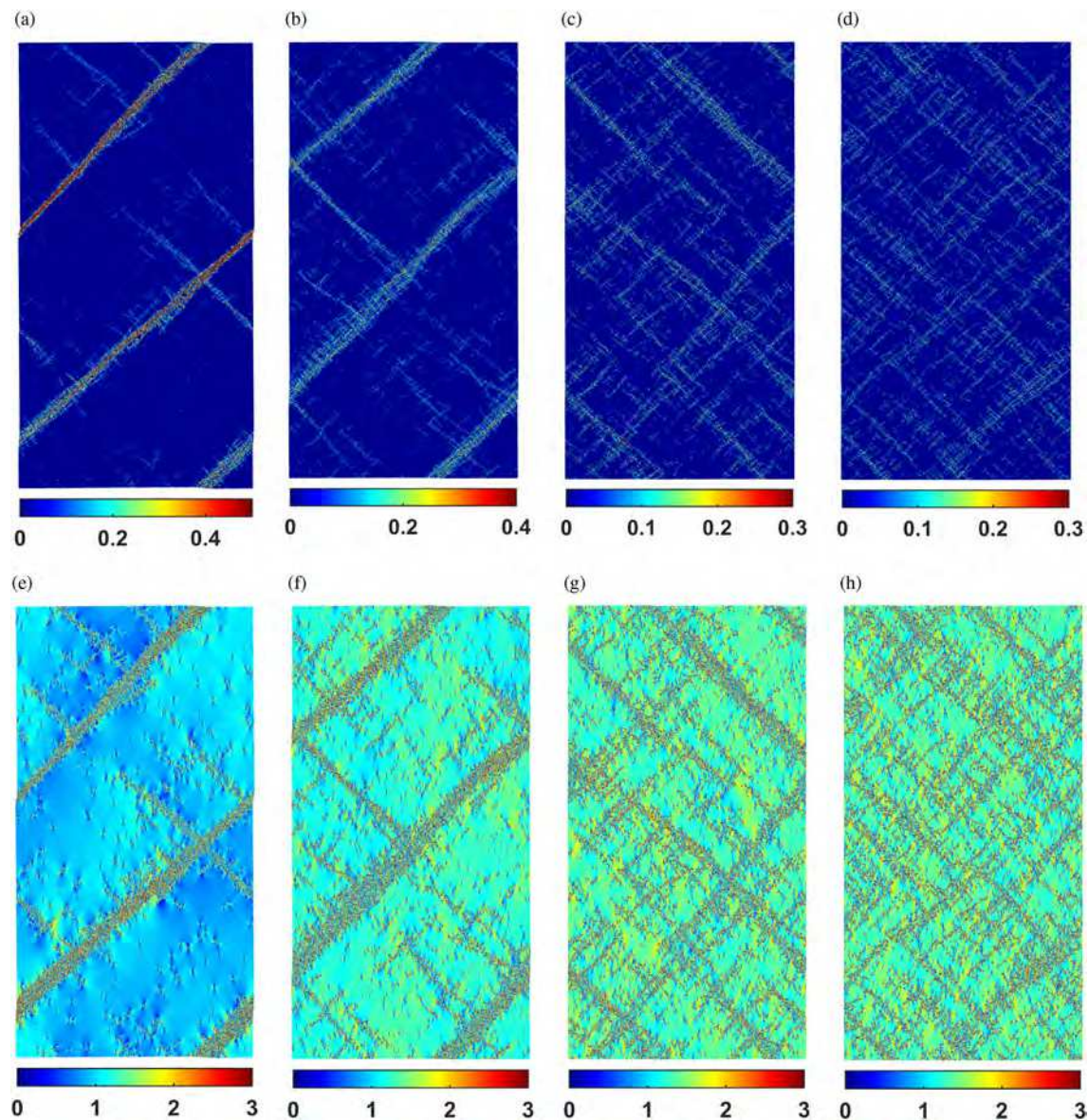
Fig. 3. Spatial distribution of von Mises equivalent strain (top row) and stress (bottom row, colorbar unit = GPa) at 2.7% elongation in MG samples with different amounts of the six-fold MROs. From left to right the six-fold STZ volume fraction is, respectively, 0%, 10%, 20%, and 30%. (The uniaxial tension is along the vertical direction.) (For interpretation of the references to colour in this figure legend, the reader is referred to the web version of this article.)
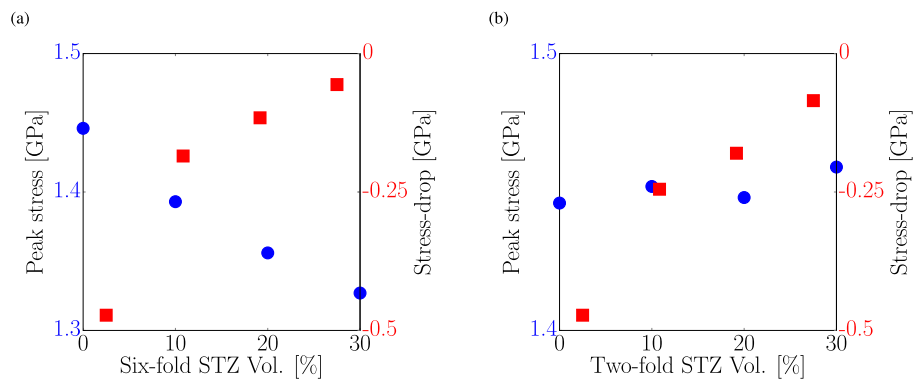

Fig. 4. Peak stress and stress-drop variation against the volume fraction of (a) six-fold and (b) two-fold STZs.

introduce another type of STZs that possess two characteristic SFTS tensors. It needs to be pointed out that it is quite possible that along other directions in the multi-dimensional strain space, there are other potential transformation modes, which, however, are located in a longer distance in the strain space as illustrated in Fig. 1. We then perform the same set of simulations as above by replacing the six-fold STZs with the two-fold STZs. The obtained tensile stress-strain curves are quite different from the ones obtained from the previous case (Fig. 2(a)), as shown in Fig. 2(b). The peak stress remains virtually the same for the samples containing different amounts of two-fold STZs and is the same as that of the homogeneous sample. This means that for a given MG sample containing initially certain amount of pseudo-FCC MROs, if annealing indeed converts these crystal-like MROs into chains of icosahedral clusters (i.e., with pseudo two-fold symmetry), with other local properties remaining more or less the same, our simulations suggest that the peak strength will increase to the level of a homogeneous sample. This result agrees with the experiments [53,54], and atomistic simulations [55] have also shown that a slow cooling rate (i.e., allowing the glass to anneal more as compared to a fast cooling rate) can significantly increase the peak-stress of glasses. Regarding the influence on shear banding, the results are similar to the case of six-fold STZs as shown in Fig. 3, that is, more two-fold STZs will lead to more diffuse shear bands.

Apart from the stress-strain curves and deformation microstructures, we can perform extreme value (EV) statistics analysis to assess the damage-tolerance. In Fig. 5(a), EV analysis for simulation results shown in Fig. 2(a) is presented. Clearly, as the amount of the crystal-like STZs increases, the "tail" of the distribution becomes shorter and shorter, implying that fewer and fewer extreme values of the local (STZ level) plastic strain are developed. More quantitatively, Fig. 5(b) plots for different Φ the volume fraction of "extreme sites", defined as voxels with accumulated transformation strain larger than 0.3 (the characteristic shear of STZ is 0.1). The decrease of extreme site population with increasing Φ suggests that by introducing more crystal-like MROs, the glass can be more damage-tolerant. In addition, we also compare the different effects on damage tolerance due to six-fold and two-fold STZs, as shown in Fig. 5(b). Except for the cases of $\Phi = 30\%$ that have a much lower amount of extreme values and lead to essentially a homogeneous deformation in either the six-fold or two-fold STZ case, samples containing two-fold STZs tend to develop much more extreme sites than samples containing six-fold STZs with the same amount. Since extreme sites are usually prone to initiation of

cracks, our results show that conversion from the pseudo-FCC MROs into the two-fold chains of icosahedral clusters may significantly reduce the damage-tolerance and render the MGs more brittle, which agrees with the annealing effect on MGs observed in the experiment [53,56].

4. Discussion

4.1. Strain frustration

The revealed correlation between the MRO-level heterogeneities and the mechanical properties of MGs originates from the available (with respect to the time scale of the applied deformation/loading increment) transformation modes of STZs, which is inherently determined by the topological features of potential energy landscape (PEL) [57,58] of the glass and reflected in our model by the number of SFTS tensors to be considered during STZ dynamics. This parameter is expected to depend on the processing history such as cooling rate, annealing or pre-deformation. The local change of MRO symmetry (via bond rearrangements between neighboring SROs, see, e.g. Ref. [59]) can produce local ordering that changes the distribution and/or population of nearest-neighbor basins. This will essentially change the available inelastic shear modes of STZs and hence alter the resulting long-range elastic energy. Quantitative PEL description of glasses and related phenomena can provide our model with detailed information of STZ shear modes but is still facing major computational challenges [58]. The current work takes directly experimentally revealed MROs and derives the corresponding STZs based on local structural ordering. The simulation results, though parametric in nature, provide a qualitative understanding of the correlation between MROs and shear banding.

Better understanding of the influence of MROs on plasticity of MGs can be achieved by considering the frustration introduced by MROs. It needs to be pointed out that the concept "frustration" has been introduced to understand liquid-glass transition and two types of frustration have been proposed, i.e., geometrical frustration [60] and energetic frustration [61]. Here we propose a concept called *strain frustration*, which is the frustration between (1) choosing the plastic mode in strain space favored by global shape change and (2) choosing the locally more favored mode that is selected from a limited set in the time scale of the applied deformation/loading increment. Glasses have inherent strain frustration when subject to an applied stress/strain due to the heterogeneous
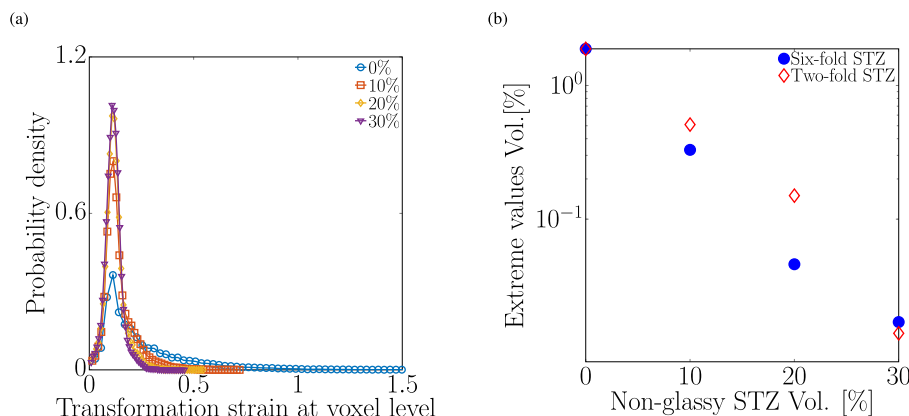

Fig. 5. (a) Probability density distribution of voxel-level accumulated transformation strains at macroscopic elongation of 2.7% in Fig. 2(a). (b) Volume fractions of extreme sites at macroscopic elongation of 2.7% in Fig. 2(a) and (b).
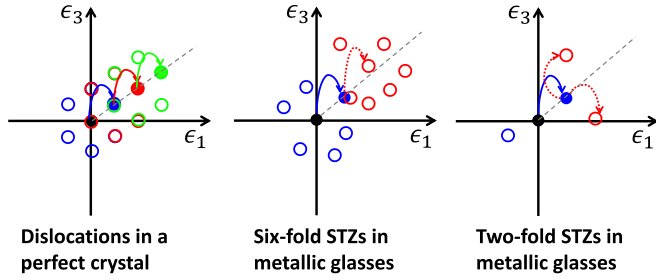
Fig. 6. Schematics of different strain frustration scenarios in perfect crystals and MGs containing either six-fold or two-fold STZs (top view of the abstracted potential energy landscape [33] in a simplified two-dimensional strain-space). The grey dashed line indicates the favored strain path by the applied deformation/loading and the lack of potential available shear modes (open circles) along this line creates strain frustration. Different generations of STZs are colored by different colors and the actual selected mode is indicated by a solid circle. A solid curve with an arrowhead indicates the actual transformation path (basin-to-basin transition) and a dotted curve the potential path. (For interpretation of the references to colour in this figure legend, the reader is referred to the web version of this article.)

shear mode catalog of STZ that are originated from the inherent atomic structure heterogeneity [33,62]. While crystals can also experience strain frustration when subject to certain orientation with respect to the applied stress (e.g., the scenario of multiple-slip), here we only consider the case where the macroscopic shape change is concordant with one of the active Burgers vectors, which serves as a clear example to illustrate the key difference between crystal and MG plasticity and the physical meaning of strain frustration. In Fig. 6, we show schematically the different strain frustration scenarios in perfect crystals and MGs containing either six-fold or two-fold STZs and it is evident that the "degree" of frustration between the local plastic behavior and global shape change is largely determined by the available STZ shear modes. In the current case, the distinctive shear catalogs for dissimilar STZs (derived from the MROs) and glassy matrix will introduce a strain frustration on top of the inherent frustration, as a dissimilar STZ (either two-fold or six-fold) tries to relax the internal stress produced by the glassy STZ that is very likely to be non-concordant with any mode in its own catalog. According to our current simulation, such additional strain frustration can serve as *intrinsic* obstacles for shear band propagation, in that the introduction of either six-fold or two-fold STZs leads to more diffuse shear bands or even homogeneous deformation. This is analogous to the "precipitation-hardening" effect in crystals (where precipitates can prevent localized shear and thus increase toughness [63–65]), with

now dissimilar STZs serving as nanoscale "precipitates" in glasses to prevent the catastrophic shear localization caused by the matrix STZs. In fact, approaches of introducing second phases in MGs essentially follow the "precipitation-hardening" philosophy as well. It can be further inferred based on our results that if certain preferential "orientation" of crystal-like MROs are produced via specific processing routes (namely, a MRO texture is introduced), the mechanical property may be changed as well.

To have a more quantitative understanding of the resulting strain frustration, we consider the characteristic angle

$$\theta(\mathbf{x}) = \frac{1}{2}\tan^{-1}\frac{2\varepsilon_3}{\varepsilon_1 - \varepsilon_2} \tag{6}$$

defined in the Mohr's circle for the 2D SFTS tensor $\varepsilon(\mathbf{x})$ of STZs as defined previously. There is also a similar angle defined by the current macroscopic shape change $\bar{\varepsilon}$, i.e.,

$$\bar{\theta} = \frac{1}{2}\tan^{-1}\frac{2\bar{\varepsilon}_3}{\bar{\varepsilon}_1 - \bar{\varepsilon}_2}. \tag{7}$$

The difference between the local and macroscopic angle,

$$\Delta\theta(\mathbf{x}) = \theta(\mathbf{x}) - \bar{\theta}, \tag{8}$$

measures the deviation of locally selected plastic mode and the globally favored mode, and is expected to possess certain distribution due to the inherent glassy heterogeneity. Since $\bar{\theta}$ is mainly determined by the applied strain, the influence of MRO-derived STZs on the plasticity is through the selection of $\theta(\mathbf{x})$ and is reflected in the *probability density function* of $\Delta\theta$. In a homogeneous sample, a STZ can always find a shear mode to effectively relax the local stress produced by other neighboring STZs due to the similar catalog with sufficiently large number of modes. As a result, the activated plastic modes of STZs within the shear band are expected to be largely dominated by the local stress states; the prescribed global shape change only needs to be satisfied in the volume-average sense, which produces virtually no strain frustration for STZ transformations. When increasing the volume fraction of dissimilar STZs, local stress relaxation within shear bands is significantly frustrated due to the distinctive shear modes of those "foreign" STZs (as illustrated in Fig. 6) and shear band propagation is effectively retarded. In other words, the "autocatalytic" effect due to transformation-induced local stress is blunted by the strain frustration due to these nanoscale "precipitates". Consequently, the subsequent plastic deformation is no longer favored (or dominated)
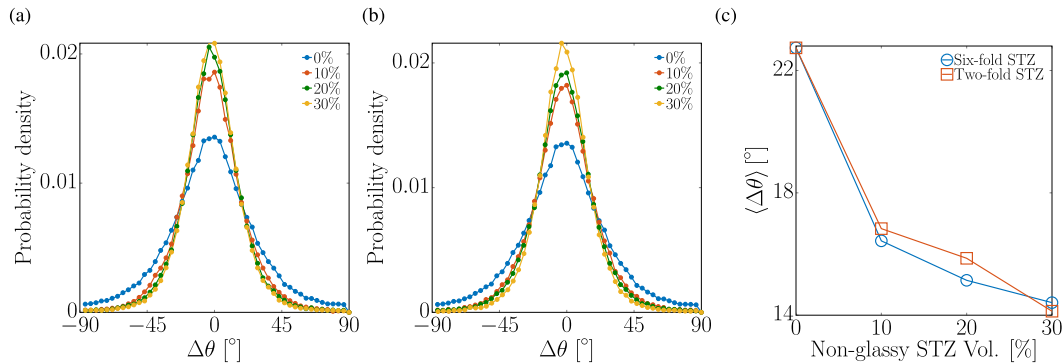

Fig. 7. (a) Probability density distribution of deviation of the characteristic angle of local STZ transformations from that of macroscopic shape change ($\Delta\theta$) at 2.8% elongation for MGs containing various volume fractions of six-fold STZs. (b) Same as (b) except for MGs containing two-fold STZs. (c) Comparison of the average value of $\Delta\theta$ for MG containing various volume fractions of either six-fold or two-fold STZs.
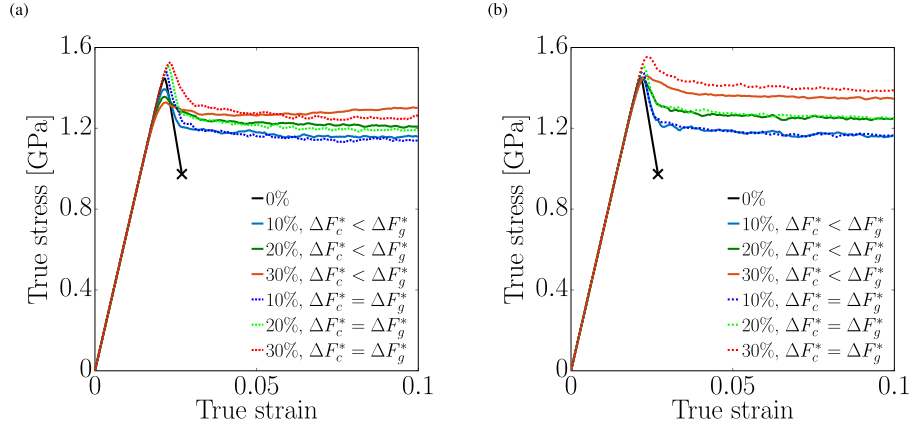
Fig. 8. Simulated tension stress-strain curves of MG samples with different volume fractions of (a) six-fold and (b) two-fold STZs with $\Delta F_c^* < \Delta F_g^*$ and $\Delta F_c^* = \Delta F_g^*$.
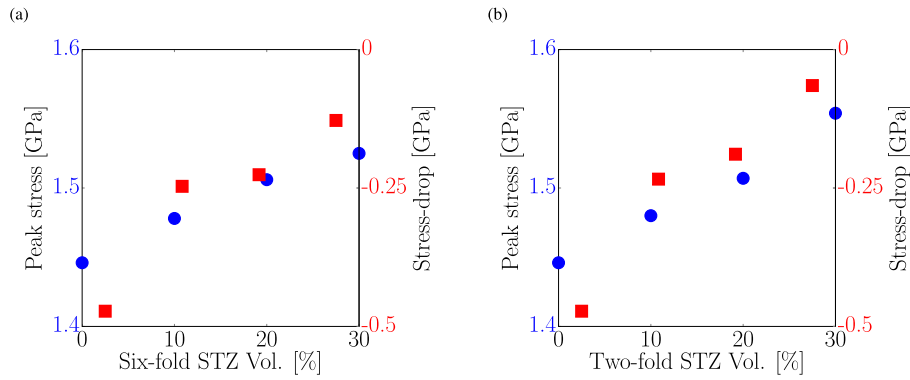

Fig. 9. Variation of the peak stress and stress-drop corresponding to the results ($\Delta F_c^* = \Delta F_g^*$) in Fig. 8 for the case of (a) six-fold and (b) two-fold STZs.

by the local stresses but rather by the global shape change that can select STZs from the entire spatial domain. This suggests that the majority of $\theta(\mathbf{x})$ will have a value close to the average $\bar{\theta}$ and consequently $\Delta\theta$ will tend to have smaller values. This is indeed confirmed by the analysis of our simulation results as shown in Fig. 7(a) and (b), where fewer STZs with larger $\Delta\theta$ are found with increasing Φ in MGs containing either six-fold or two-fold STZs.

Regarding the different influence of the six-fold and two-fold STZs on plasticity, the difference in the probability density distribution of $\Delta\theta(\mathbf{x})$ in MGs containing either the six-fold or two-fold STZs (at a given Φ) is difficult to perceive by a direct comparison using Fig. 7(a) and (b). We thus compare the average of the absolute value of $\Delta\theta(\mathbf{x})$, i.e.,

$$\langle \Delta\theta \rangle \equiv \langle |\Delta\theta(\mathbf{x})| \rangle_{\mathbf{x}}, \tag{9}$$

which gives a measure of the average deviation between the local and global deformation modes, and the result is shown in Fig. 7(c). It may suggest that the introduction of the two-fold STZs tends to, on average, promote a slightly larger $\Delta\theta$ as compared to that of MGs containing the six-fold STZs. This has in fact been indicated by the schematics shown in Fig. 6, which suggests that the two-fold STZs tend to introduce more significant strain frustration than the six-fold STZs and consequently the two-fold STZs can be considered plastically "harder" than the six-fold STZs statistically. In other words, the stress state produced by an arbitrary glassy STZ is more likely to be relaxed by a six-fold STZ before it can be relaxed by a two-fold STZ due to the limited shear modes of the latter, i.e., a larger degree of strain frustration. As a result, a higher stress level is

required to trigger the transformation of two-fold STZs as compared to that of six-fold STZs, even though the activation energy barrier for the two are the same in our simulations. When the six-fold STZs are all replaced by the two-fold STZs, the glass requires a higher macroscopic stress level to yield. If such stress is equal to or higher than the yield strength of a homogeneous sample, then the material may start to yield in the matrix first but the two-fold STZs still serve as the obstacle (precipitate) to impede shear band propagation. The macroscopic yield strength in this case will remain the same, which corresponds to our current simulations. It is also interesting to note that Fig. 7(c) exhibits similar features as those shown in Fig. 5(b), which actually resembles the well-known strength-ductility trade-off in many crystals, that is, the increase of the strength (measured here by $\Delta\theta$ in Fig. 7(c)) is accompanied by the decrease of the ductility (or equivalently, the increase of brittleness, measured by the volume fraction of extreme values in Fig. 5(b)).

4.2. Effect of activation energetics of MROs

The heterogeneous nature of the glass structure is expected to lead to non-uniform local properties. Indeed, experimentally, it has been shown that the local elastic properties in MGs can exhibit significant variation on a scale below 10 nm [66]. For the inelastic deformation properties considered in this work, the activation energy barrier of crystal-like STZs, ΔF_c^*, is assumed to be smaller than that of glassy STZs, ΔF_g^* (Section 2). As has been mentioned in Section 2.2, this is a theoretical assumption based on the fact that
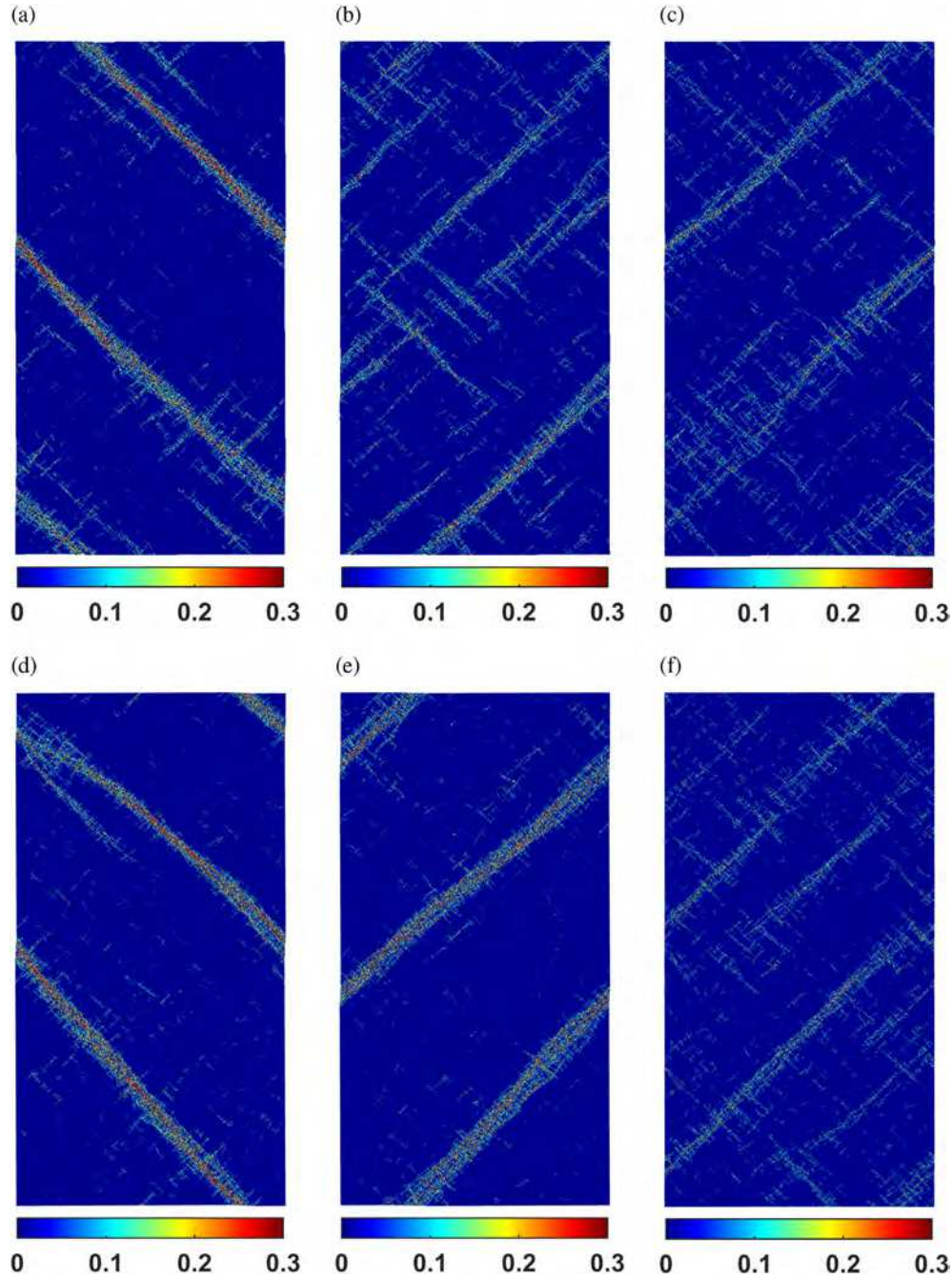
Fig. 10. Spatial distribution of von Mises equivalent strain at 2.7% elongation in MG samples with different amounts of the six-fold (top row) and two-fold (bottom row) MROs with $\Delta F_c^* = \Delta F_g^*$. From left to right the six-fold STZ volume fraction is, respectively, 10%, 20%, and 30%. (The uniaxial tension is along the vertical direction.)

local crystalline order of MROs may facilitate slip along preferential directions more readily (for example, with much lower Peierls stress) due to the inherent local translational symmetry, which is, however, not present in the 5-fold icosahedra. Nevertheless, the absolute value of ΔF_c^* and ΔF_g^* can only be unambiguously obtained from atomistic simulations [67,68] for a given MG system, and it is likely that the relationship between ΔF_c^* and ΔF_g^* can be more complex and perhaps system-dependent as well.

To see the effect of ΔF_c^* on the shear banding dynamics before realistic and large-scale atomistic simulations of the MRO struc-

tures become available, we carry out an additional set of simulations using $\Delta F_c^* = \Delta F_g^*$ to compare with the results in Section 3. The simulated stress-strain curves are shown in Fig. 8 for different volume fractions of the crystal-like STZs (for comparison, results of Fig. 2 for $\Delta F_c^* < \Delta F_g^*$ is also plotted), and the variation of the corresponding peak stress and stress-drop are shown in Fig. 9.

As compared with the result of $\Delta F_c^* < \Delta F_g^*$ (Figs. 2 and 4), a clear difference is that the peak stress increases as the volume fraction of the crystal-like STZs increases for both cases of six-fold and two-fold STZs. This is consistent with the above analysis of strain

frustration introduced by the crystal-like STZs. Regarding the stress-drop, the results in Fig. 9 are similar to those in Fig. 4, namely, more crystal-like STZs lead to less stress-drop post peak stress. This is actually an indication of more diffuse shear bands, which is confirmed by examining the strain and strain distribution as shown in Fig. 10.

In addition, we also fix the volume fraction of the crystal-like STZs to be 30% and carry out another simulation with $\Delta F_c^* = 5$ eV $> \Delta F_g^*$, of which the simulated stress-strain curve is compared in Fig. 11, together with the previous results, and the corresponding shear banding is plotted in Fig. 12. If the crystal-like STZs are more difficult to activate, plastic deformation will simply be accommodated primarily by the glassy matrix, and as long as the crystal-like STZs remain as the minority and distributed randomly in space without clustering, shear bands can form easily and percolate throughout the matrix.
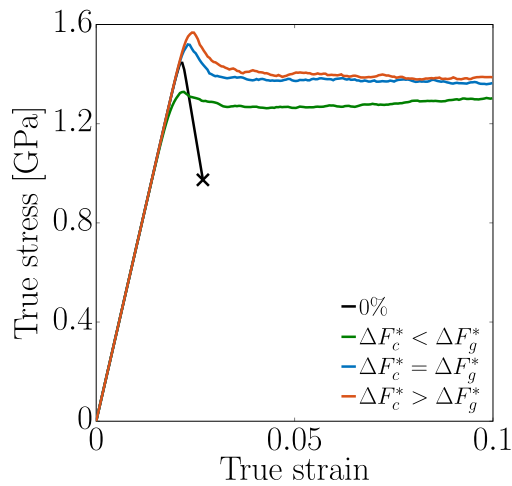

Fig. 11. Effect of activation energy barrier on simulated tension stress-strain curves of MG samples with 30% volume fractions of six-fold STZs.

4.3. Strain hardening due to MROs

One feature in Fig. 11 is that noticeable strain hardening is present for the sample containing 30% volume fraction of the six-fold STZs, but not in any other samples simulated. While the current model does not consider any failure mechanism, the simulated strain hardening may still reflect some inherent plastic features due to STZ dynamics and is thus worth some discussion. In fact, the strain hardening starts around 3% macroscopic strain (Fig. 11), close to the experimentally measured elastic limit of many MGs [48].

After examining the strain distribution for all simulations, it is found that the sample containing 30% volume fraction of the six-fold STZs exhibits a homogeneous flow virtually throughout the elongation, while the others all exhibit certain degrees of localization. As an example, Fig. 13 plots the strain distribution after 10% elongation of three samples containing (i) 30% volume fractions of the six-fold STZs, (ii) 20% volume fractions of the six-fold STZs, and (iii) 30% volume fractions of the two-fold STZs. It is seen clearly that plastic flow in sample-(i) is homogeneous. With either the volume faction of the six-fold STZs decreasing to 20%, i.e., sample-(ii), or the type of crystal-like STZs changing to two-fold, i.e., sample-(iii), plastic flow becomes localized to certain degrees. In fact, this homogeneous nature of plastic flow in sample-(i) can be seen at the early stage when plasticity is just initiated (2.7% elongation), as shown in Fig. 3(d). If STZ activation is localized in space, i.e., forming a shear band, the subsequent STZ activation will primarily be at/near the interface between the shear band and undeformed matrix due to stress concentration, or within the existing shear band due to inherent softening [33]. As a result, no strain hardening should be expected when the glass deform via the formation of a dominant shear band, as confirmed by the current simulations as well as our previous work [33]. As dissimilar STZs can act as "precipitates" to prevent the formation of a dominant shear band (Section 4.1), plastic flow can be homogeneous when sufficient number of dissimilar STZs are present. Subsequent STZ activation will thus need to overcome the back stress that is present everywhere in this homogeneously deformed sample (similar to the back stress for dislocation glide exerted by coherent precipitates in many
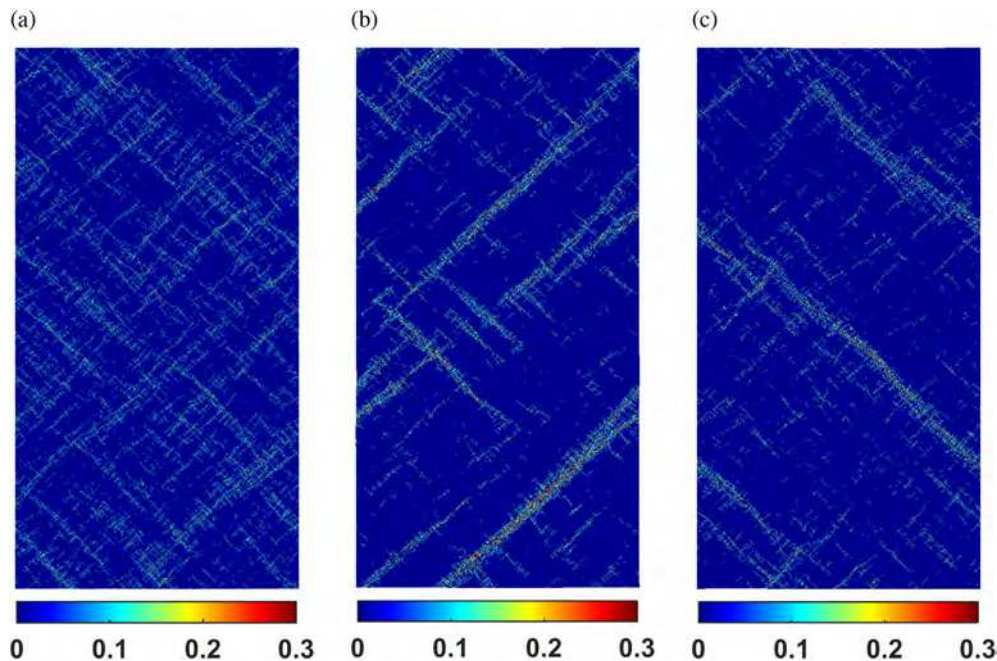

Fig. 12. Spatial distribution of von Mises equivalent strain at 2.7% elongation in MG samples with 30% volume fractions of six-fold STZs using (a) $\Delta F_c^* < \Delta F_g^*$, (b) $\Delta F_c^* = \Delta F_g^*$, and (c) $\Delta F_c^* > \Delta F_g^*$.

engineering alloys), which leads to the observed strain hardening in sample-(i). The reason why sample-(iii) does not show strain hardening is related to the different degree of strain frustration induced by the six-fold and two-fold STZs as discussed in Section 4.1; essentially, because the two-fold STZs require higher stress to activate as compared to the six-fold STZs, the former are not as effective as the latter to diffuse shear localization (particular at the early stage of plastic deformation) as confirmed by our simulations.

5. Conclusions

In summary, experimentally revealed crystal-like MROs in MGs are correlated with dissimilar STZs that possess a set of shear transformation modes related to the packing symmetry of the underlying MROs. STZ dynamics simulations show that glasses containing dissimilar STZs derived from the MROs form much more diffuse shear bands during deformation as compared to glasses
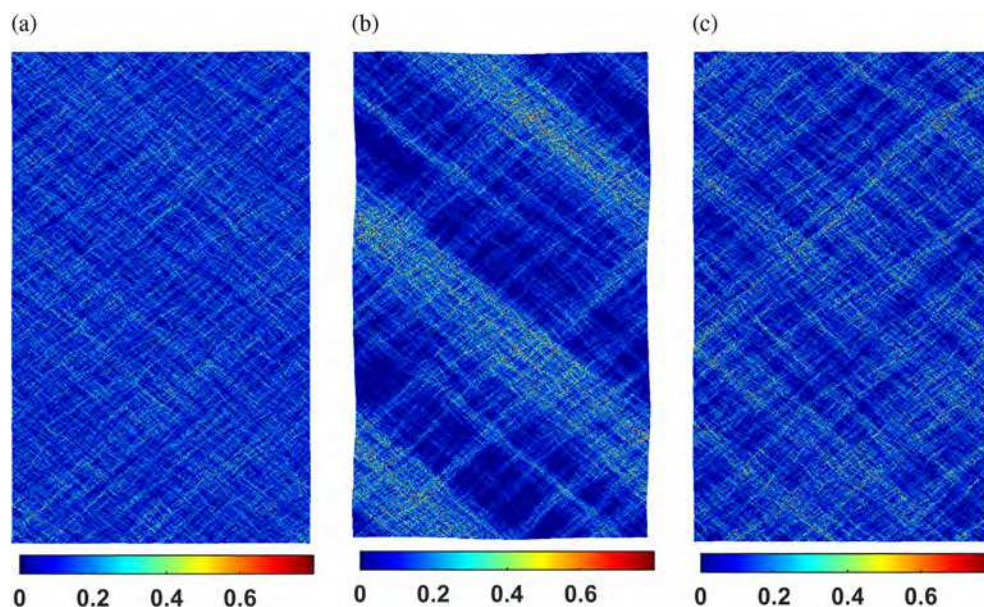

Fig. 13. Spatial distribution of von Mises equivalent strain at 10% elongation in MG samples with (a) 30% volume fractions of six-fold STZs, (b) 20% volume fractions of six-fold STZs, and (c) 30% volume fractions of two-fold STZs.

4.4. Outlook

The fixed ΔF^* assumed for the crystal-like STZs is expected to be valid if we focus mainly on the early stage of plasticity. As extensive plastic deformation occurs, local heating can occur [69] and may also erase the aging history (also known as "rejuvenation") [55]. Consequently, the MROs may be able to evolve as suggested by annealing experiments [14] and even nanocrystals can form as suggested by many experiments [70–72]. This suggests that in reality the energetics of different STZs/MROs can be more complicated and may evolve upon thermal/mechanical loading. More understanding of the nature of MROs such as the local structural and chemical information are required to formulate a model for the transitions between different MROs, which is certainly an interesting aspect to consider and can be incorporated in our model in future studies. Nevertheless, argument, analysis, and concept based on the current parametric studies should remain valid and meaningful.

In addition, more accurate experimental measurement such as the size and spatial distribution of MROs can also be incorporated in our model to study the resulting effect on plastic deformation of MGs. Recently, an amorphous/nanocrystalline dual-phase structure has been synthesized and shown to exhibit significant suppression of the formation of a dominant shear band owing to the embedded nanocrystals with sizes below 10 nm [44], which is similar to what has been demonstrated (but with structural heterogeneities at a different length scale) in our current simulations. With more detailed information of MROs available from experiments and atomistic simulations, our model can provide more quantitative prediction of the influence of MROs on the mechanical behavior of MGs.

containing less nanoscale structural heterogeneity. A "precipitation-hardening" effect is observed by introducing these dissimilar STZs in MGs. Different shear transformation characteristics of the dissimilar STZs can lead to distinctive "strain-frustration" and thus different mechanical properties as well, which may be correlated with the influence of transitions between different MROs due to thermal/mechanical processes. Extreme statistics analysis suggests that increasing the amount of MROs may lead to a more damage-tolerant glass, and the type of MROs may also influence the ductility. The current work indicates the important role played by the structural heterogeneity at the MRO-level and suggests a new scheme to design MGs with intrinsic ductility.

Acknowledgments

References

[1] C. Hays, C. Kim, W.L. Johnson, Microstructure controlled shear band pattern formation and enhanced plasticity of bulk metallic glasses containing in situ formed ductile phase dendrite dispersions, Phys. Rev. Lett. 84 (2000) 2901.

[2] C. Fan, R. Ott, T. Hufnagel, Metallic glass matrix composite with precipitated ductile reinforcement, Appl. Phys. Lett. 81 (2002) 1020–1022.

[3] D.C. Hofmann, J.-Y. Suh, A. Wiest, G. Duan, M.-L. Lind, M.D. Demetriou, W.L. Johnson, Designing metallic glass matrix composites with high toughness and tensile ductility, Nature 451 (2008) 1085–1089.

[4] S. Pauly, S. Gorantla, G. Wang, U. Kühn, J. Eckert, Transformation-mediated ductility in cuzr-based bulk metallic glasses, Nat. Mater. 9 (2010) 473–477.

[5] Y. Wu, Y. Xiao, G. Chen, C.T. Liu, Z. Lu, Bulk metallic glass composites with transformation-mediated work-hardening and ductility, Adv. Mater. 22 (2010) 2770–2773.

[6] Y. Wang, J. Li, A.V. Hamza, T.W. Barbee, Ductile crystalline–amorphous

nanolaminates, Proc. Natl. Acad. Sci. 104 (2007) 11155–11160.

[7] B.J. Park, H.J. Chang, D.H. Kim, W.T. Kim, K. Chattopadhyay, T. Abinandanan, S. Bhattacharyya, Phase separating bulk metallic glass: a hierarchical composite, Phys. Rev. Lett. 96 (2006) 245503.

[8] J. Schroers, C. Veazey, M.D. Demetriou, W.L. Johnson, Synthesis method for amorphous metallic foam, J. Appl. Phys. 96 (2004) 7723–7730.

[9] D.B. Miracle, A structural model for metallic glasses, Nat. Mater. 3 (2004) 697–702.

[10] H. Sheng, W. Luo, F. Alamgir, J. Bai, E. Ma, Atomic packing and short-to-medium-range order in metallic glasses, Nature 439 (2006) 419–425.

[11] D. Ma, A.D. Stoica, X.-L. Wang, Power-law scaling and fractal nature of medium-range order in metallic glasses, Nat. Mater. 8 (2009) 30–34.

[12] M. Wakeda, Y. Shibutani, Icosahedral clustering with medium-range order and local elastic properties of amorphous metals, Acta Mater. 58 (2010) 3963–3969.

[13] Y. Cheng, E. Ma, Atomic-level structure and structure–property relationship in metallic glasses, Prog. Mater. Sci. 56 (2011) 379–473.

[14] J. Hwang, Z. Melgarejo, Y. Kalay, I. Kalay, M. Kramer, D. Stone, P. Voyles, Nanoscale structure and structural relaxation in zr 50 cu 45 al 5 bulk metallic glass, Phys. Rev. Lett. 108 (2012) 195505.

[15] P. Zhang, J.J. Maldonis, M. Besser, M. Kramer, P.M. Voyles, Medium-range structure and glass forming ability in zr–cu–al bulk metallic glasses, Acta Mater. 109 (2016) 103–114.

[16] H. Shintani, H. Tanaka, Frustration on the way to crystallization in glass, Nat. Phys. 2 (2006) 200–206.

[17] H. Tanaka, T. Kawasaki, H. Shintani, K. Watanabe, Critical-like behaviour of glass-forming liquids, Nat. Mater. 9 (2010) 324–331.

[18] P. Murali, U. Ramamurty, Embrittlement of a bulk metallic glass due to sub-t g annealing, Acta Mater. 53 (2005) 1467–1478.

[19] M. Falk, J. Langer, Dynamics of viscoplastic deformation in amorphous solids, Phys. Rev. E 57 (1998) 7192.

[20] S. Mayr, Activation energy of shear transformation zones: a key for understanding rheology of glasses and liquids, Phys. Rev. Lett. 97 (2006) 195501.

[21] D. Pan, A. Inoue, T. Sakurai, M. Chen, Experimental characterization of shear transformation zones for plastic flow of bulk metallic glasses, Proc. Natl. Acad. Sci. 105 (2008) 14769–14772.

[22] J. Puthoff, J. Jakes, H. Cao, D. Stone, Investigation of thermally activated deformation in amorphous pmma and zr-cu-al bulk metallic glasses with broadband nanoindentation creep, J. Mater. Res. 24 (2009) 1279–1290.

[23] A. Argon, Plastic deformation in metallic glasses, Acta Metall. 27 (1979) 47–58.

[24] Y. Shi, M.L. Falk, Strain localization and percolation of stable structure in amorphous solids, Phys. Rev. Lett. 95 (2005) 095502.

[25] C.A. Schuh, T.C. Hufnagel, U. Ramamurty, Mechanical behavior of amorphous alloys, Acta Mater. 55 (2007) 4067–4109.

[26] J.S. Harmon, M.D. Demetriou, W.L. Johnson, K. Samwer, Anelastic to plastic transition in metallic glass-forming liquids, Phys. Rev. Lett. 99 (2007) 135502.

[27] H. Yu, W. Wang, H. Bai, Y. Wu, M. Chen, Relating activation of shear transformation zones to β relaxations in metallic glasses, Phys. Rev. B 81 (2010) 220201.

[28] C.H. Rycroft, E. Bouchbinder, Fracture toughness of metallic glasses: annealing-induced embrittlement, Phys. Rev. Lett. 109 (2012) 194301.

[29] M.L. Manning, A.J. Liu, Vibrational modes identify soft spots in a sheared disordered packing, Phys. Rev. Lett. 107 (2011) 108302.

[30] J. Ding, S. Patinet, M.L. Falk, Y. Cheng, E. Ma, Soft spots and their structural signature in a metallic glass, Proc. Natl. Acad. Sci. 111 (2014) 14052–14056.

[31] Y. Wang, M. Li, J. Xu, Toughen and harden metallic glass through designing statistical heterogeneity, Scr. Mater. 113 (2016) 10–13.

[32] E.R. Homer, C.A. Schuh, Mesoscale modeling of amorphous metals by shear transformation zone dynamics, Acta Mater. 57 (2009) 2823–2833.

[33] P. Zhao, J. Li, Y. Wang, Heterogeneously randomized stz model of metallic glasses: softening and extreme value statistics during deformation, Int. J. Plasticity 40 (2013) 1–22.

[34] L. Li, E. Homer, C. Schuh, Shear transformation zone dynamics model for metallic glasses incorporating free volume as a state variable, Acta Mater. 61 (2013) 3347–3359.

[35] P. Zhao, J. Li, Y. Wang, Extended defects, ideal strength and actual strengths of finite-sized metallic glasses, Acta Mater. 73 (2014) 149–166.

[36] W.G. Stratton, J. Hamann, J.H. Perepezko, P.M. Voyles, X. Mao, S.V. Khare, Aluminum nanoscale order in amorphous al 92 sm 8 measured by fluctuation electron microscopy, Appl. Phys. Lett. 86 (2005) 141910.

[37] H. Nitsche, F. Sommer, E. Mittemeijer, The al nano-crystallization process in amorphous al 85 ni 8 y 5 co 2, J. non-crystalline solids 351 (2005) 3760–3771.

[38] M.C. Gao, F. Guo, S.J. Poon, G.J. Shiflet, Development of fcc-al nanocrystals in al–ni–gd metallic glasses during continuous heating dsc scan, Mater. Sci. Eng. A 485 (2008) 532–543.

[39] J. Perepezko, S. Imhoff, R. Hebert, Nanostructure development during devitrification and deformation, J. Alloys Compd. 495 (2010) 360–364.

[40] A. Sadoc, O. Heckmann, V. Nassif, O. Proux, J.-L. Hazemann, L. Xing, K. Kelton, Local order and nanostructure induced by microalloying in al–y–fe amorphous alloys, J. Non-Crystalline Solids 353 (2007) 2758–2766.

[41] Y. Sun, F. Zhang, Z. Ye, Y. Zhang, X. Fang, Z. Ding, C.-Z. Wang, M.I. Mendelev, R.T. Ott, M.J. Kramer, et al., Crystal genes in metallic liquids and glasses, Sci. Rep. 6 (2016).

[42] R.J. Hebert, Nanocrystals in Metallic Glasses, INTECH Open Access Publisher, 2011.

[43] E. Ma, Tuning order in disorder, Nat. Mater. 14 (2015) 547–552.

[44] G. Wu, K.-C. Chan, L. Zhu, L. Sun, J. Lu, Dual-phase nanostructuring as a route to high-strength magnesium alloys, Nature 545 (2017) 80–83.

[45] C. Bennett, P. Chaudhari, V. Moruzzi, P. Steinhardt, On the stability of vacancy and vacancy clusters in amorphous solids, Philos. Mag. A 40 (1979) 485–495.

[46] A.R. Yavari, A. Le Moulec, A. Inoue, N. Nishiyama, N. Lupu, E. Matsubara, W.J. Botta, G. Vaughan, M. Di Michiel, Å. Kvick, Excess free volume in metallic glasses measured by x-ray diffraction, Acta Mater. 53 (2005) 1611–1619.

[47] F. Shimizu, S. Ogata, J. Li, Yield point of metallic glass, Acta Mater. 54 (2006) 4293–4298.

[48] W. Johnson, K. Samwer, A universal criterion for plastic yielding of metallic glasses with a (t/t g) 2/3 temperature dependence, Phys. Rev. Lett. 95 (2005) 195501.

[49] P. Zhao, S. Im, J. Hwang, Y. Wang, New insights into deformation of metallic glasses by combining mesoscale simulation and fluctuation electron microscopy, Microsc. Microanal. 22 (2016) 1436–1437.

[50] S. Sun, B. Adams, W. King, Observations of lattice curvature near the interface of a deformed aluminium bicrystal, Philos. Mag. A 80 (2000) 9–25.

[51] J. Hwang, P. Voyles, Variable resolution fluctuation electron microscopy on cu-zr metallic glass using a wide range of coherent stem probe size, Microsc. Microanal. 17 (2011) 67–74.

[52] G. Kumar, T. Ohkubo, T. Mukai, K. Hono, Plasticity and microstructure of zr–cu–al bulk metallic glasses, Scr. Mater. 57 (2007) 173–176.

[53] J.J. Lewandowski, Effects of annealing and changes in stress state on fracture toughness of bulk metallic glass, Mater. Trans. 42 (2001) 633–637.

[54] J. Lewandowski, W. Wang, A. Greer, Intrinsic plasticity or brittleness of metallic glasses, Philos. Mag. Lett. 85 (2005) 77–87.

[55] M. Utz, P.G. Debenedetti, F.H. Stillinger, Atomistic simulation of aging and rejuvenation in glasses, Phys. Rev. Lett. 84 (2000) 1471.

[56] U. Ramamurty, M. Lee, J. Basu, Y. Li, Embrittlement of a bulk metallic glass due to low-temperature annealing, Scr. Mater. 47 (2002) 107–111.

[57] F.H. Stillinger, T.A. Weber, Packing Structures and Transitions in Liquids and Solids, vol. 225, Science, Washington, DC, 1984, pp. 983–989.

[58] P.G. Debenedetti, F.H. Stillinger, Supercooled liquids and the glass transition, Nature 410 (2001) 259–267.

[59] Y. Suzuki, J. Haimovich, T. Egami, Bond-orientational anisotropy in metallic glasses observed by x-ray diffraction, Phys. Rev. B 35 (1987) 2162.

[60] G. Tarjus, S.A. Kivelson, Z. Nussinov, P. Viot, The frustration-based approach of supercooled liquids and the glass transition: a review and critical assessment, J. Phys. Condens. Matter 17 (2005) R1143.

[61] H. Tanaka, Two-order-parameter description of liquids. i. a general model of glass transition covering its strong to fragile limit, J. Chem. Phys. 111 (1999) 3163–3174.

[62] D. Srolovitz, V. Vitek, T. Egami, An atomistic study of deformation of amorphous metals, Acta Metall. 31 (1983) 335–352.

[63] J. Staley, Microstructure and Toughness of High-strength Aluminum Alloys, in: Properties Related to Fracture Toughness, ASTM International, 1976.

[64] P. Gregson, H. Flower, Microstructural control of toughness in aluminium-lithium alloys, Acta Metall. 33 (1985) 527–537.

[65] J.W. Martin, Precipitation Hardening: Theory and Applications, Butterworth-Heinemann, 2012.

[66] H. Wagner, D. Bedorf, S. Küchemann, M. Schwabe, B. Zhang, W. Arnold, K. Samwer, Local elastic properties of a metallic glass, Nat. Mater. 10 (2011) 439–442.

[67] F. Shimizu, S. Ogata, J. Li, Theory of shear banding in metallic glasses and molecular dynamics calculations, Mater. Trans. 48 (2007) 2923–2927.

[68] D. Rodney, C. Schuh, Distribution of thermally activated plastic events in a flowing glass, Phys. Rev. Lett. 102 (2009) 235503.

[69] J. Lewandowski, A. Greer, Temperature rise at shear bands in metallic glasses, Nat. Mater. 5 (2006) 15–18.

[70] H. Chen, Y. He, G. Shiflet, S. Poon, Deformation-induced nanocrystal formation in shear bands of amorphous alloys, Nature 367 (1994) 541–543.

[71] W. Jiang, M. Atzmon, The effect of compression and tension on shear-band structure and nanocrystallization in amorphous al 90 fe 5 gd 5: a high-resolution transmission electron microscopy study, Acta Mater. 51 (2003) 4095–4105.

[72] C.-C. Wang, Y.-W. Mao, Z.-W. Shan, M. Dao, J. Li, J. Sun, E. Ma, S. Suresh, Real-time, high-resolution study of nanocrystallization and fatigue cracking in a cyclically strained metallic glass, Proc. Natl. Acad. Sci. 110 (2013) 19725–19730.